Near field intensity pattern at the output of silica-based graded-index multimode fibers under selective excitation with a single-mode fiber

Near-field intensity pattern at the output of silica-based graded-index multimode fibers under selective excitation with a single-mode fiber

C. P. Tsekrekos, R. W. Smink, B. P. de Hon, A. G. Tijhuis, and A. M. J. Koonen

COBRA Research Institute, Eindhoven University of Technology, Den Dolech 2, P. O. Box 513, 5600 MB Eindhoven, The Netherlands

c.tsekrekos@tue.nl; r.w.smink@tue.nl

Abstract: Selective excitation of graded-index multimode fibers (GI-MMFs) with a single-mode fiber (SMF) has gained increased interest for telecommunication applications. It has been proposed as a way to enhance the transmission bandwidth of GI-MMF links and/or create parallel communication channels over the same GI-MMF. Although the effect of SMF excitation on the transmission bandwidth has been investigated, its impact on the near-field intensity pattern at the output face of the GI-MMF has not been systematically addressed. We have carried out an analysis of the near-field intensity pattern at the output face of silica-based GI-MMFs excited by a radially offset SMF. Simulation results exhibit all of the features displayed by experimental ones. It turns out that differential mode attenuation and delay, full intra-group mode mixing, and small deviations in the refractive index profile of the GI-MMF do not affect the overall shape of the near-field intensity, which is determined by the radial offset of the input SMF. This can be exploited in mode group diversity multiplexing links. The effect of defects in the refractive index profile, such as a central dip or peak, is also examined.

OCIS codes: (060.2330) Fiber optics communications; (060.4230) Multiplexing; (350.5500) Propagation.

References and links

1. Z. Haas and M. A. Santoro, "A Mode-filtering scheme for improvement of the bandwidth-distance product in Multimode Fiber Systems," J. Lightwave Technol. **11**, 1125-1131 (1993).
2. M. Düser and P. Bayvel, "2.5 Gbit/s transmission over 4.5 km of 62.5 μm multimode fibre using centre launch technique," Electron. Lett. **36**, 57-58 (2000).
3. S. S.-H. Yam and F. Achten, "Single wavelength 40 Gbit/s transmission over 3.4 km broad wavelength window multimode fibre," Electron. Lett. **42**, 592-593 (2006).
4. L. Raddatz, I. H. White, D. G. Cunningham, and M. C. Nowell, "An Experimental and theoretical study of the offset launch technique for the enhancement of the bandwidth of multimode fiber links," J. Lightwave Technol. **16**, 324-331 (1998).
5. L. Raddatz and I. H. White, "Overcoming the Modal Bandwidth Limitation of Multimode Fiber by using Pass-band Modulation," IEEE Photon. Technol. Lett. **11**, 266-268 (1999).
6. K. M. Patel, A. Polley, K. Balemarthy, and S. E. Ralph, "Spatially resolved detection and equalization of modal dispersion limited multimode fiber links," J. Lightwave Technol. **24**, 2629-2636 (2006).

#79384 - $15.00 USD Received 24 January 2007; revised 14 March 2007; accepted 15 March 2007

7. H. R. Stuart, "Dispersive Multiplexing in Multimode Optical Fiber," Science **289**, 281-283 (2000).
8. T. Koonen, H. van den Boom, I. Tafur Monroy, and G.-D. Khoe, "High capacity multi-service in-house networks using mode group diversity multiplexing," in *Optical Fiber Communication Conference*, Technical Digest (CD) (Optical Society of America, 2004), paper FG4.
9. A. R. Shah, R. C. J. Hsu, A. Tarighat, A. H. Sayed, and B. Jalali, "Coherent Optical MIMO (COMIMO)," J. Lightwave Technol. **23**, 2410-2419 (2005).
10. P. L. Neo and T. D. Wilkinson, "Holographic Implementation of Optical Multiple-Inputs, Multiple-Outputs (MIMO) on a Multimode Fiber," in *Conference on Lasers and Electro-Optics/Quantum Electronics and Laser Science Conference and Photonic Applications Systems Technologies*, Technical Digest (CD) (Optical Society of America, 2006), paper CMNN2.
11. C. P. Tsekrekos, A. Martinez, F. M. Huijskens, and A. M. J. Koonen, "Design considerations for a transparent mode group diversity multiplexing link," IEEE Photon. Technol. Lett. **18**, 2359-2361 (2006).
12. M. Wegmuller, S. Golowich, G. Giaretta, and M. Nuss, "Evolution of the beam diameter in a multimode fiber link through offset connectors," IEEE Photon. Technol. Lett. **13**, 574-576 (2001).
13. C. K. Asawa and H. F. Taylor, "Propagation of light trapped within a set of lowest-order modes of graded-index multimode fiber undergoing bending," Appl. Opt. **39**, 2029-2037 (2000).
14. S. Schöllmann and W. Rosenkranz, "Experimental investigations of mode coupling as limiting effect using mode group diversity multiplexing on GI-MMF," in *Proceedings of European Conference on Optical Communications*, Sep. 2006, paper We3.P.87.
15. A. M. J. Koonen, "Bit-Error-Rate Degradation in a Multimode Fiber Optic Transmission Link due to Modal Noise," IEEE J. Sel. Areas Commun. **SAC-4**, 1515-1522 (1986).
16. D. Gloge and E. A. J. Marcatili, "Multimode Theory of Graded-Core Fibers," Bell Syst. Tech. J. **52**, 1563-1578 (1973).
17. A. W. Snyder and J. D. Love, *Optical Waveguide Theory*, (Chapman and Hall, 1983).
18. A. H. Cherin, *An Introduction to Optical Fibers*, (McGraw-Hill, 1983).
19. S. Kawakami and H. Tanji, "Evolution of Power Distribution in Graded-Index Fibres," Electron. Lett. **19**, 100-102 (1983).
20. G. Yabre, "Comprehensive Theory of Dispersion in Graded-Index Optical Fibers," J. Lightwave Technol. **18**, 166-177 (2000).
21. M. Bingle and B. P. de Hon, "Differential Mode Delay Full-wave modeling and various levels of approximations," in Proceedings of the General XXVIIth Assembly of the International Union of Radio Science, Aug. 2002, paper 2060.
22. J. G. Dil and H. Blok, "Propagation of Electromagnetic Surface Waves in a Radially Inhomogeneous Optical Waveguide," Opto-electronics **5**, 415-428 (1973).
23. Y. Daido, E. Miyauchi, T. Iwama, and T. Otsuka, "Determination of modal power distribution in graded-index optical waveguides from near-field patterns and its application to differential mode attenuation measurement," Appl. Opt. **18**, 2207-2213 (1979).
24. O. G. Leminger and G. K. Grau, "Near-Field Intensity and Modal Power Distribution in Multimode Graded-index Fibers," Electron. Lett. **16**, 678-679 (1980).
25. M. Rousseau and L. Jeunhomme, "Optimum index profile in multimode optical fiber with respect to mode coupling," Opt. Commun. **23**, 275-278 (1977).
26. M. Webster, L. Raddatz, I. H. White, and D. G. Cunningham, "A Statistical analysis of conditioned launch for gigabit ethernet links using multimode fiber," J. Lightwave Technol. **17**, 1532-1541 (1999).
27. http://www.ieee802.org/3/aq/public/tools/
28. http://www.ieee802.org/3/aq/public/tools/108fiberModel/CamMMF1p2/CamMMF1p2%20Supplement.pdf

1. Introduction

In in-building and campus optical networks, silica-based graded-index multimode fiber (GI-MMF) is widely used. The short range of these networks, typically up to 300 m and maximally up to 1 km, has originally allowed GI-MMF to support the bandwidth needs. In addition, the large core diameter of the GI-MMF, compared to the single-mode fiber (SMF), offers installation and handling benefits. The rapid developments in multimedia and data-based services have led to an increased demand in bandwidth. GI-MMF links are based on the intensity modulation (IM), direct-detection (DD), single-input single-output (SISO) transmission approach. In this case, the bandwidth limitation comes from inter-modal dispersion, which is caused by the differential propagation delay of the propagating spatial modes.

One way to enhance the 3-dB bandwidth of IM-DD SISO links with GI-MMF is to restrict the launch conditions, aiming at the excitation of a subset of modes with similar propagation

#79384 - $15.00 USD Received 24 January 2007; revised 14 March 2007; accepted 15 March 2007

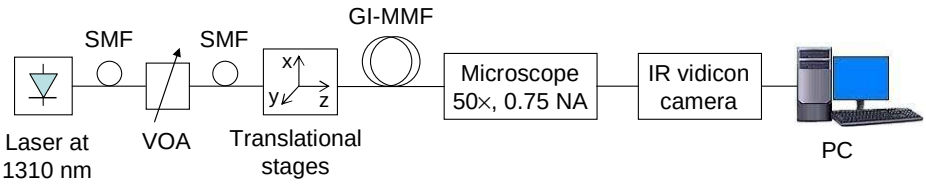

Fig. 1. Experimental setup for the observation of the NFP at the output of a GI-MMF under selective excitation with a radially offset SMF.

delay. Selective excitation with an SMF at the input face of a GI-MMF is a simple way to achieve this [1–4]. A radial offset at the launch position of the SMF with respect to the GI-MMF axis may be required, depending on the refractive index profile of the GI-MMF. Central launch can be combined with detectors for SMF links offering a similar advantage. Subcarrier multiplexing beyond the 3-dB bandwidth [5] and spatially resolved equalization [6] can also enhance the transmission bandwidth of GI-MMF links.

Besides the above methods, multiple-input multiple-output (MIMO) techniques are gaining interest to create parallel channels over the same MMF, by exploiting the propagating spatial modes [7–10]. In all MIMO approaches, selective excitation is required. Mode group diversity multiplexing (MGDM) [8], in particular, is an IM-DD MIMO technique that can be implemented with radially offset Gaussian-like beams at the input face of a GI-MMF and spatially selective detection of the optical power at the GI-MMF output [11]. This implementation is based on the experimental observation that for silica-based GI-MMFs, at least up to 1-km long, the near-field pattern (NFP) of the optical intensity at the GI-MMF output is confined within a disk with a radius that depends on the radial offset of the input beam.

The analysis presented in this paper has been motivated by the aforementioned interest in selective excitation of GI-MMFs with an SMF. The effect of such an excitation scheme on the bandwidth of IM-DD SISO links has been widely addressed [1–4]. Although its effect on the NFP has been observed experimentally [11–14], no extended analysis has been reported, to the best of the authors' knowledge. In this paper, we present an experimental and theoretical investigation of the NFP. We show that the overall NFP is not affected by differential mode delay and attenuation, small deviations in the refractive index profile of the GI-MMF, or full intra-group mode mixing. The latter refers to mixing among modes with similar propagation coefficient, as it will be explained below. Further, we examine the effect of refractive index profile defects, such as a central dip or peak. This analysis gives insight into light propagation in silica-based GI-MMFs and finds direct application in MGDM links.

2. Experimental investigation

Figure 1 shows the experimental setup used to observe the NFP at the output of a GI-MMF under selective excitation. An external cavity type tunable semiconductor laser was used to excite selectively a GI-MMF with core/cladding diameter of 62.5/125 μm and central numerical aperture (NA) 0.275. The linewidth of the laser is 85 kHz and its wavelength was tuned to 1310 nm. The laser is pigtailed with a 1-m long standard SMF. A variable optical attenuator (VOA) with SMF pigtails was used to control the level of the optical power. The radial offset of the SMF axis from the GI-MMF axis was set by means of computer-controlled translational stages. A microscope with $50\times$ magnification and NA $= 0.75$ projected the NFP at the GI-MMF output onto an infra-red vidicon camera. An image of the NFP was grabbed with video processing software.

#79384 - $15.00 USD Received 24 January 2007; revised 14 March 2007; accepted 15 March 2007

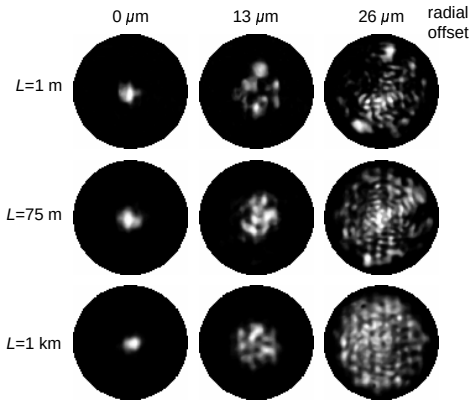

Fig. 2. Experimental NFP at the output of a 1-m, 75-m and 1-km long 62.5/125 μm silica-based GI-MMF, under selective excitation with a radially offset SMF. The radial offset was 0, 13 and 26 μm.

The obtained NFP images are shown in Fig. 2. Three GI-MMFs were tested, of lengths 1 m, 75 m and 1 km, under excitation with the SMF of the VOA at 0, 13 and 26 μm radial offset. The speckle contrast of the images is very strong even in the case of the 1-km long GI-MMF. This is due to the very narrow linewidth of the laser that results in highly coherent radiation [15]. Similar results have been previously obtained at 660 nm [11], 850 nm [12], 1300 nm [13], and 1540 nm [14]. The images of Fig. 2 indicate that propagation does not affect the overall NFP, which remains confined within a disk. The radial offset of the SMF determines the radius of the disk. This indicates that mode mixing is limited, since in the presence of strong mode mixing, light would span most of the area of the GI-MMF core and the radial dependence of the intensity profile would tend to resemble the refractive index profile [16]. To investigate the impact of separate propagation effects as well as of the refractive index profile on the NFP, numerical simulations are required.

3. Numerical investigation

Important effects in MMFs are dispersion, attenuation and mode mixing. Inter-modal dispersion is usually the dominant source of dispersion. Chromatic dispersion depends on the wavelength and the linewidth of the optical source. In our experiment, we used a 1310-nm laser with an 85-kHz linewidth and therefore chromatic dispersion can be neglected. We employ cylindrical polar coordinates r, ϕ, z, with the z-axis coinciding with the MMF axis. At the MMF input $z = 0$, whereas at the MMF output $z = L$. The propagating electric $\mathbf{E}$ and magnetic $\mathbf{H}$ fields are [17]

$$\begin{bmatrix} \mathbf{E}(r,\phi,z,t) \\ \mathbf{H}(r,\phi,z,t) \end{bmatrix} = \sum_{\nu,\mu} c_{\nu,\mu}(z) \begin{bmatrix} \mathbf{e}_{\nu,\mu}(r,\phi) \\ \mathbf{h}_{\nu,\mu}(r,\phi) \end{bmatrix} exp(\mathrm{j}\omega t). \quad (1)$$

Here, $\mathbf{e}_{\nu,\mu}$, $\mathbf{h}_{\nu,\mu}$ are the modal electric and magnetic fields of the (ν,μ) guided mode, where ν and μ are the azimuthal and radial mode numbers. The modal fields $\mathbf{e}_{\nu,\mu}(r,\phi)$, $\mathbf{h}_{\nu,\mu}(r,\phi)$ are normalized to unit power and $c_{\nu,\mu}(z)$ is the complex modal amplitude at z, its modulus expressing the fractional modal power. Further, ω is the optical angular frequency.

#79384 - $15.00 USD Received 24 January 2007; revised 14 March 2007; accepted 15 March 2007

The intensity distribution at the MMF output is given by

$$I(r,\phi,L)=\frac{1}{2}Re\left[\sum_{\nu,\mu}\mathbf{e}_{\nu,\mu}(r,\phi,L)\times\mathbf{h}^{*}_{\nu,\mu}(r,\phi,L)\cdot\hat{u_z}+\sum_{\substack{\nu\neq\nu'\\ \mu\neq\mu'}}\mathbf{e}_{\nu,\mu}(r,\phi,L)\times\mathbf{h}^{*}_{\nu',\mu'}(r,\phi,L)\cdot\hat{u_z}\right]. \tag{2}$$

On the right hand side of Eq. (2), the first term is the summation of the intensity distributions due to each mode separately and the second term expresses the variations in the total intensity distribution due to the interference of the modal fields.

In the absence of mode mixing, we have

$$c_{\nu,\mu}(z)=c_{\nu,\mu}(0)exp(-\mathrm{j}\beta_{\nu,\mu}z)exp(-\gamma_{\nu,\mu}z), \tag{3}$$

where $\beta_{\nu,\mu}$, $\gamma_{\nu,\mu}$ are the propagation and attenuation coefficients of the (ν,μ) mode. We assume that losses are limited, so that they can be treated as a perturbation of the lossless case [17]. The modal amplitudes in the plane of excitation, $c_{\nu,\mu}(0)$, depend on the excitation condition. In particular, the orthogonality of the modal fields at $z=0$ reads

$$c_{\nu,\mu}(0)=\int_0^{2\pi}\int_0^{\infty}\mathbf{e}_{in}(r,\phi)\times\mathbf{h}^{*}_{\nu,\mu}(r,\phi)\cdot\hat{u}_z r\mathrm{d}r\mathrm{d}\phi \tag{4}$$

where $\mathbf{e}_{in}(r,\phi)$ is the excitation electric field at the MMF input.

Mode mixing is the gradual redistribution of the optical power among the propagating modes. It can be separated in two categories. Intra-group and inter-group mode mixing, referring to mixing among modes of the same principal mode group (PMG), and among modes of different PMGs, respectively. PMGs consist of modes whose propagation coefficient is very similar. Under the weakly guiding approximation, the modes that constitute a PMG are the degenerate (ν,μ) modes of the linearly polarized $\mathrm{LP}_{\ell,\mu}$ modes with LP mode number $M_{\mathrm{LP}}=\ell+2\mu$, where ℓ is related to ν [18]. In silica-based GI-MMFs, mode mixing is limited, with intra-group mixing occurring earlier than inter-group mixing [19]. For our analysis, we consider the effect of full intra-group mode mixing, as a case of practical importance. We calculate the total power launched in a PMG and redistribute it evenly among the modes of the PMG. In other words, the modulus of the amplitudes $c^{m}_{\nu,\mu}(L)$ of all modes in the mth PMG will be

$$\left|c^{m}_{\nu,\mu}(L)\right|=\sqrt{\frac{\sum_{\nu,\mu}\left|c^{m}_{\nu,\mu}(0)\right|^2}{N_m}}, \tag{5}$$

where N_m is the number of modes in the mth PMG. The phase of $c^{m}_{\nu,\mu}(L)$ is chosen randomly with a uniform distribution over $[0,2\pi)$.

The modal field distributions $\mathbf{e}_{\nu,\mu}(r,\phi)$, $\mathbf{h}_{\nu,\mu}(r,\phi)$ and the propagation coefficients $\beta_{\nu,\mu}$ depend on the wavelength and the refractive index profile $n(r)$. We assume that $n(r)$ follows the well-known power-law profile, i.e.,

$$n(r)=\begin{cases} n_0\sqrt{1-2\Delta\left(\frac{r}{a}\right)^{\alpha}}, & r<a,\\ n_0\sqrt{1-2\Delta}, & r\geq a,\end{cases} \tag{6}$$

where $\Delta=[n_0^2-n^2(a)]/(2n_0^2)$ and a is the GI-MMF core radius. The central NA of the GI-MMF is $\mathrm{NA}=n_0\sqrt{2\Delta}$. For our simulations, $n_0=1.474$ and $\mathrm{NA}=0.275$. The α-parameter was 1.97, 2 and 2.06. The value $\alpha=2$ corresponds to the parabolic index profile. For $\alpha=1.97$ and $\alpha=2.06$

#79384 - $15.00 USD Received 24 January 2007; revised 14 March 2007; accepted 15 March 2007

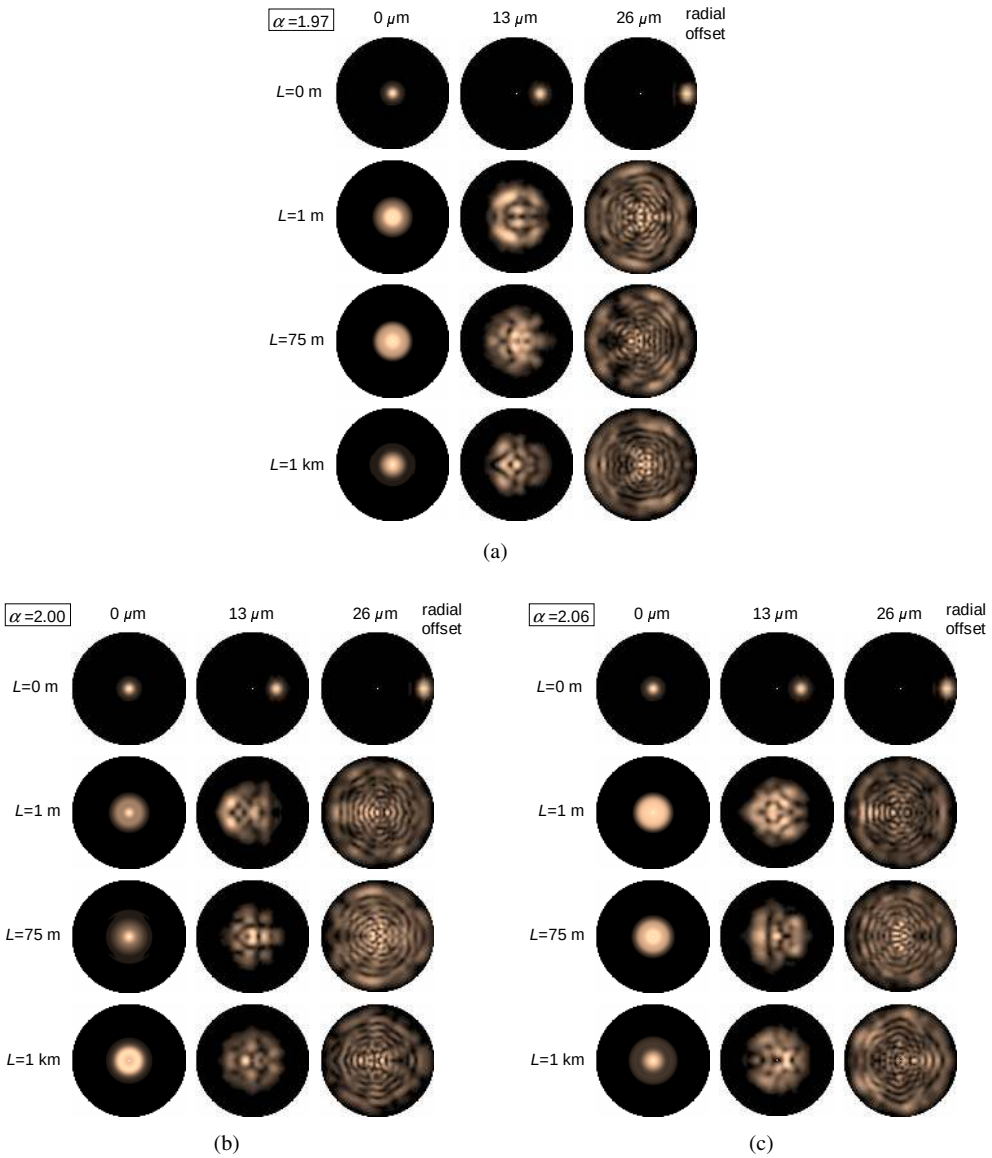

Fig. 3. Simulated NFP at the output of a 62.5/125 μm silica-based GI-MMF with refractive index parameter (a) $\alpha = 1.97$, (b) $\alpha = 2$ and (c) $\alpha = 2.06$. Each row corresponds to a different GI-MMF length (L) and each column to a different radial offset of the input SMF. Mode mixing is not taken into account.

differential mode delay is minimized at 1300 and 850 nm wavelength, respectively [20, 21], and therefore these values are of special interest in the design of GI-MMFs. To account for the radial dependency of the refractive index in the core, the computation of the propagation coefficients $\beta_{\nu,\mu}$ and the modal fields $\mathbf{e}_{\nu,\mu}(r,\phi)$, $\mathbf{h}_{\nu,\mu}(r,\phi)$ is performed by a direct numerical integration of Maxwell's equations in their full-wave form [22]. Models based on ray optics can be also used to give the near-field intensity yielded by a mode group, however, excitation of a large number of modes is assumed and the phase of the modal amplitudes is not taken into

#79384 - $15.00 USD Received 24 January 2007; revised 14 March 2007; accepted 15 March 2007

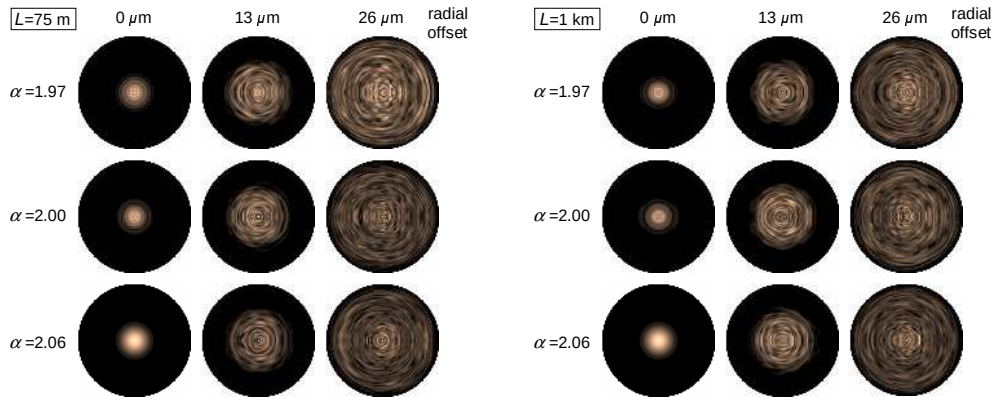

Fig. 4. Simulated NFP at the output of a (a) 75-m (b) 1-km long 62.5/125 μm silica-based GI-MMF, assuming full intra-group mode mixing. Each row corresponds to a different refractive index parameter (α) and each column to a different radial offset of the input SMF.

consideration [23, 24].

The following relation can be used to give the attenuation coefficients,

$$\gamma_m(\lambda) = \gamma_0(\lambda) + \gamma_0(\lambda) I_9 \left[7.35 \left(\frac{m-1}{M_0} \right)^{2\alpha/(\alpha+2)} \right], \tag{7}$$

where I_9 is the 9th-order modified Bessel function of the first kind. This relation has been proposed in Ref. [20] using experimental data from Ref. [25]. According to Eq. (7) differential mode attenuation becomes significant in higher order modes. λ is the wavelength and $\gamma_0(\lambda)$ the attenuation of the lowest-order mode which travels the shortest optical path. At 1310 nm it corresponds to 0.35 dB/km. M_0 is the total number of PMGs. The value of $\gamma_m(\lambda)$ depends on m and therefore is the same for all modes in the mth PMG. Consequently, in the calculation of $exp(-\gamma_{\nu,\mu} z)$ in Eq. (3), when full intra-group mode mixing is considered, we may take $z = L$ for all modes.

The results of the simulated NFPs are shown in Figs. 3 and 4. Figure 3 illustrates the NFP considering differential mode attenuation and delay, but not taking into account mode mixing. The mode field diameter of the input SMF was 9.3 μm and its radial offset was 0, 13 and 26 μm. The NFP was calculated for $L = 0$, 1, 75 m and $L = 1$ km. Figure 3(a) corresponds to $\alpha = 1.97$, Fig. 3(b) to $\alpha = 2$ and Fig. 3(c) to $\alpha = 2.06$. The speckle pattern clearly depends on the refractive index profile. However, in all three cases of the index profile, the overall NFP is confined within a disk with a radius that depends on the offset of the input SMF, but not on the α-parameter. It should be noted that although the values of the α-parameter used in the simulations have no significant effect on the overall NFP, they can strongly influence the GI-MMF bandwidth [20]. In Fig. 4, full intra-group mode mixing is taken into account. The same offsets of the input SMF and the same index profiles are considered. The NFP is shown at the output of a 75-m and a 1-km long GI-MMF. Full intra-group mixing does not change the overall NFP either. A distinct difference between the images of Figs. 3 and 4 is that in the case of Fig. 4, the speckle contrast is less strong. This is related to the phase of $c^m_{\nu,\mu}(L)$ which is taken randomly in the results of Fig. 4. The effect is similar to that of incoherent radiation that would yield a very smooth NFP. Both Figs. 3 and 4 show that differential mode attenuation does not influence the overall NFP, even in the case of an input beam with a radial offset of 26 μm,

#79384 - $15.00 USD Received 24 January 2007; revised 14 March 2007; accepted 15 March 2007

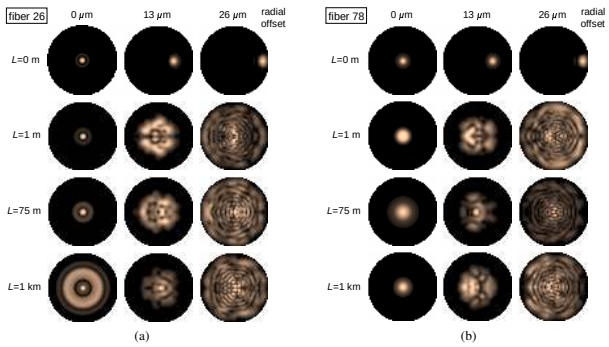

Fig. 5. Simulated NFP at the output of a 62.5/125 μm silica-based GI-MMF using (a) fiber 26 and (c) fiber 78 from the 108-fiber model. Each row corresponds to a different GI-MMF length (L) and each column to a different radial offset of the input SMF. Mode mixing is not taken into account.

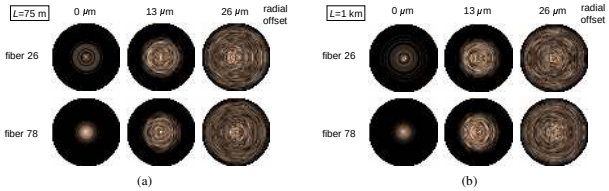

Fig. 6. Simulated NFP at the output of a (a) 75-m (b) 1-km long 62.5/125 μm silica-based GI-MMF, assuming full intra-group mode mixing. Each row corresponds to a different refractive index profile and each column to a different radial offset of the input SMF.

where light propagates primarily in higher order modes. Our simulations give symmetric NFP images. This is due to the symmetric excitation field, since the polarization of the input beam was set in the radial direction of the GI-MMF. In principle, the NFP is not symmetric. This approach, though, has the practical advantage of reducing the computational time, since only half of the NFP has to be simulated.

4. Refractive index profile defects

In the preceding section, we presented simulation results of the NFP at the output face of silica-based GI-MMFs. Three different refractive index profiles were tested. These profiles follow the well-known power-law relation and each profile is characterized by a different parameter α. One profile corresponds to the parabolic one, while the other two are of great interest in the manufacturing of high-quality silica GI-MMFs, as the GI-MMF used in our experiment. However, the refractive index profile of field installed GI-MMFs may have stronger defects than a simple variation of the parameter α. Such defects are included in the 108-fiber model introduced in Ref. [26] and expanded by the IEEE 802.3aq committee [27]. In this section, we use two fibers from the 108-fiber model, namely fibers 26 and 78. The refractive index profile of fiber 26 has a central (on-axis) dip, while the profile of fiber 78 shows a central peak. Beyond the central part of the fiber, the refractive index is divided in two regions, each described by a different parameter α. In fibers 26 and 78, the differences in the values of α in these two regions are the largest assured differences in the 108-fiber set, viz. $\alpha = 1.89$ and $\alpha = 2.05$. Fibers 26 and 78 also include a kink perturbation in the profile at 27 μm and 19 μm distance from the GI-MMF axis, correspondingly. More detailed description of the 108-fiber model, including

#79384 - $15.00 USD Received 24 January 2007; revised 14 March 2007; accepted 15 March 2007

fibers 26 and 78 can be found in Ref. [28].

The simulation results are shown in Figs. 5 and 6, considering no mode mixing and full intra-group mode mixing, respectively. The speckle patterns in the NFPs are different compared to the ones in Figs. 3 and 4. However, the overall NFP is affected only when fiber 26 is used with central excitation. In this case, the NFP can expand significantly and span over an area similar to the area of the NFP yielded by the 13 μm offset input beam. This will affect an MGDM link, and if such a fiber would be used, central excitation should be avoided. The results obtained with fiber 78 are very similar to the ones in Figs. 3 and 4 for all input beams.

5. Conclusions

In this paper, experimental and simulation results of the NFP at the output of silica-based GI-MMFs have been presented and compared. Selective excitation with a radially offset SMF has been considered. The NFP is confined within a disk, the radius of which depends on the radial offset of the input SMF. It has been shown that differential mode delay and attenuation, as well as full intra-group mode mixing do not change the overall NFP, although they do affect the speckle pattern. The same holds for small deviations of the refractive index profile. This supports the proposition that MGDM links can be tolerant as regards the GI-MMF length [11]. Finally, it has been shown that when the refractive index profile exhibits a central dip, the overall NFP under central excitation can significantly expand, while in the case of a central peak, the overall NFP remains practically intact. Therefore, in an MGDM link over a GI-MMF with a central dip, on-axis excitation should be avoided.

Acknowledgment

The authors would like to thank Dr. P. Matthijsse (Draka Comteq) for providing the silica GI-MMFs. Funding from the Freeband Impulse Programme of the Ministry of Economic Affairs of the Netherlands in the project Mode Group Diversity Multiplexing is gratefully acknowledged.

#79384 - $15.00 USD Received 24 January 2007; revised 14 March 2007; accepted 15 March 2007